Geminate Recombination of *n*-Butyl Isocyanide to Myoglobin†

Joseph H. Sommer, Eric R. Henry, and James Hofrichter*

Laboratory of Chemical Physics, National Institute of Arthritis, Diabetes, and Digestive and Kidney Diseases, National Institutes of Health, Bethesda, Maryland 20205

Received March 25, 1985

ABSTRACT: Transient optical absorption spectra of myoglobin were measured following photolysis of the *n*-butyl isocyanide complex with 10-ns laser pulses at room temperature. The data were analyzed by using singular value decomposition to give the kinetics of ligand rebinding and spectral changes. Geminate recombination phases were observed at 30 ns and 1 μs following photodissociation. These processes were accompanied by simultaneous changes in the shape of the Soret band which indicate changes in protein conformation. These spectral changes are not present in the geminate recombination of photolyzed complexes of myoglobin with the diatomic ligands oxygen and carbon monoxide. This difference in behavior, as well as the slower overall association rate of *n*-butyl isocyanide to myoglobin, can be rationalized as arising from distortion of the protein structure by the larger isocyanide ligand along the binding pathway.

One of the simplest protein–ligand reactions is the binding of oxygen to myoglobin. Consequently, the kinetics of binding of ligands to myoglobin have been studied in considerable detail by using a variety of techniques, including optical absorption (Antonini & Brunori, 1971; Austin et al., 1975; Hasinoff, 1977, 1981; Duddell et al., 1980; Beece et al., 1980; Cornelius et al., 1981, 1983; Reynolds et al., 1981; Reynolds & Rentzepis, 1982; Martin et al., 1982, 1983; Henry et al., 1983), infrared absorption (Alben et al., 1982), resonance Raman (Friedman et al., 1982), extended X-ray absorption fine structure (EXAFS)[1] (Chance et al., 1983), X-ray crystallography (Frauenfelder et al., 1979), and theoretical simulations (Case & Karplus, 1979). The binding and dissociation pathways have been studied primarily by using laser photolysis with laser pulse widths varying from about 250 fs (Martin et al., 1983) to several microseconds. In this experiment an intense laser pulse photodissociates the ligand from the heme iron. The recombination of the ligand is then monitored by using optical absorption, taking advantage of the large differences in extinction coefficient for the Soret band between the liganded and unliganded states of the heme chromophore.

Most of the information on the detailed binding mechanism has come from the low-temperature studies of Frauenfelder and co-workers using microsecond laser pulses (Austin et al., 1975; Beece et al., 1980; Doster et al., 1982). From extensive single wavelength measurements over a wide range of times (2 μs to 1000 s), temperatures (2–300 K), and solvent viscosities (1–10^5 cP), they have proposed a five-species model in which the ligand encounters a series of barriers in its path into and out of the protein (Austin et al., 1975; Beece et al., 1980):

$$\underset{A}{MbCO} \rightleftharpoons \underset{B}{Mb{:}CO} \rightleftharpoons \underset{C}{Mb{::}CO} \rightleftharpoons \underset{D}{Mb{:::}CO} \rightleftharpoons \underset{E}{Mb} + CO \quad (1)$$

In this model, A is myoglobin with CO covalently bound to the heme iron (MbCO), B, C, and D represent species in which the CO is still inside the protein, but not bound to the heme iron, and E is deoxymyoglobin (Mb) with the ligand in the solvent. At temperatures below 160 K the solvent is a glass, and the photodissociated ligand does not leave the protein. The rebinding curve is independent of the free ligand concentration and highly nonexponential. The shape of the rebinding curve has been interpreted as arising from a distribution of protein conformations for state B with different activation barriers for the process B → A (Austin et al., 1975). Between 160 and 200 K process B → A still dominates the observed rebinding curve, but the kinetics are too fast to be resolved by using conventional flash-photolysis techniques. At intermediate temperatures (200–260 K) the cryosolvent is a liquid, and both a ligand concentration-independent geminate rebinding phase and a bimolecular rebinding phase are observed. The geminate phase is decidely nonexponential, and its amplitude increases with increasing solvent viscosity and decreasing temperature (Beece et al., 1980). The rebinding kinetics under these conditions have been interpreted in terms of the multiple-well model described in eq 1, with sequential processes corresponding to B → A, C → A, and D → A all contributing to the rebinding curve. More recently, Doster et al. (1982) have reclassified states C and D as containing the ligand in the "protein matrix". Because the rates associated with the C → A and D → A processes are highly dependent on solvent composition and viscosity, it is not clear that they can be definitively assigned as arising from rebinding of ligands from the protein. It is possible that diffusion of ligands in the highly viscous solvent is sufficiently slow to contribute to the geminate rebinding which has been assigned to these "matrix" processes (Henry et al., 1983). State B, on the other hand, is considered to have the dissociated ligand still bound in the heme pocket. At room temperature only a single bimolecular rebinding phase was observed.

More recent studies using improved time resolution show two or more ligand rebinding phases at room temperature for both oxygen (Duddell et al., 1980; Sommer et al., 1983) and carbon monoxide (Henry et al., 1983). The more rapid phases, with relaxation times less than 1 μs, are due to geminate recombination, i.e., rebinding of the ligand to the heme iron from which it was photodissociated. For oxymyoglobin (MbO_2) two such geminate phases have been detected—a very

† This paper is dedicated to the memory of Dr. Giovanni Lipari.

* Author to whom correspondence should be addressed.

[1] Abbreviations: EXAFS, extended X-ray absorption fine structure; Mb, deoxymyoglobin; MbCO, (carbonmonoxy)myoglobin; BuNC, *n*-butyl isocyanide; MbBuNC, the *n*-butyl isocyanide complex of myoglobin; MbO_2, oxymyoglobin; SVD, singular value decomposition; OD, optical density; fwhm, full width at half-maximum.

0006-2960/85/0424-7380$01.50/0

rapid phase with a relaxation time of 100 ps and a yield of about 80% (Martin et al., 1982) and a second phase with a relaxation time of 55 ns involving rebinding to about 27% of the remaining unliganded hemes (Duddell et al., 1980). For MbCO a single geminate phase has been observed, with a relaxation time of 180 ns and a yield of 4% (Henry et al., 1983). Comparison of the data on nanosecond and longer time scales for the two ligands using the three-species model

$$\underset{1}{\mathrm{MbCO}} \underset{k_{21}}{\overset{k_{12}}{\rightleftharpoons}} \underset{2}{\mathrm{Mb{:}CO}} \underset{k_{32}}{\overset{k_{23}}{\rightleftharpoons}} \underset{3}{\mathrm{Mb + CO}} \qquad (2)$$

indicated that the difference in geminate properties and the 30-fold more rapid overall association rate for oxygen are largely due to more rapid binding at the heme ($2 \rightarrow 1$) by oxygen (Henry et al., 1983). The correspondence between the room temperature and low-temperature results is not yet clear and will have to await a detailed study over a wide temperature range that is not limited by the time resolution of the measurements. Extrapolation of the low-temperature MbCO rebinding data to room temperature using the sequential model predicts geminate yields a factor of about 10 smaller than the observed yield, arising primarily from the $C \rightarrow A$ and $D \rightarrow A$ processes. On the basis of this result, Dlott et al. (1983) have suggested that the geminate phase observed for MbCO in the room temperature experiments corresponds to the $C \rightarrow A$ and $D \rightarrow A$ (or "matrix") processes and that the $B \rightarrow A$ process is subnanosecond and not resolved in these experiments. Experiments using picosecond lasers failed to detect any geminate recombination of CO between 10 ps (the pulse width) and 10 ns (Cornelius et al., 1981), but the sensitivity of the measurements was too low to detect a geminate yield which is less than about 10%.

The overall association and dissociation rates for alkyl isocyanide binding to a number of heme proteins, including myoglobin, were recently analyzed in a detailed study by Mims et al. (1983). In an attempt to account for some of the protein-independent contributions which vary from one ligand to another, they compared the association rates and equilibrium constants for the binding of each ligand to the proteins with the corresponding parameters measured for the binding of the same ligand to a model heme dissolved in a detergent micelle. Both the association rates and the binding constants to the model heme in the micelle increased with ligand size, while the dissociation constants were size independent. This result was ascribed to unfavorable interactions between the alkyl side chains and the aqueous solvent which increase with alkyl chain length, causing the ligand to partition preferentially into the micelle (Olson et al., 1983). In contrast, the equilibrium constants and association rate constants for the binding of isocyanides to myoglobin, to hemoglobin, and to isolated hemoglobin α and β chains did not show any simple systematic dependence on the ligand size. Mims et al. (1983) interpreted most of the differences between the binding constants of the protein and heme–micelle systems as arising from direct interactions between residues on the distal side of the heme pocket, particularly the distal histidine, and the bulky ligand. These interactions would be expected to decrease both the rate of ligand binding at the heme and the equilibrium affinity, in accordance with the experimental observations. Mims et al. (1983) further suggested that the decrease in the relative binding rate with ligand size may result from a decrease in the rate at which the bulky ligands move through the protein.

To further explore the geminate processes in myoglobin, we have investigated the kinetics of ligand rebinding and conformational changes following photodissociation of *n*-butyl isocyanide (BuNC) at room temperature using 10-ns laser pulses. BuNC is a bulky ligand with six non-hydrogen atoms and allows a first look at the effect of ligand size on the geminate processes. By measuring absorption spectra through the entire Soret region with high precision, we have been able to resolve the kinetics of spectral changes arising from conformational changes, as well as the kinetics of the much larger spectral changes which result from ligand rebinding.

Materials and Methods

BuNC was purchased from Aldrich. Mass spectroscopy of this water-white liquid showed that all detectable isocyanide had the *n*-butyl side chain. An ~3% triethylamine impurity was also detected. This material was used without further purification. For the lowest BuNC concentrations, we observed an ~20% decrease in the amplitude of the photolyzed-minus-unphotolyzed difference spectrum during the 4-h course of an experiment. This change was also observed in the static spectra taken before and after the photolysis experiment, demonstrating that BuNC is not stable in aqueous solution. For this reason, the concentration of free BuNC in experiments in which the ligand concentration was varied was determined from the bimolecular rebinding rate by using the value for the bimolecular rate constant of 2.7×10^4 M^{-1} s^{-1}, determined by using freshly prepared samples.

Sperm whale skeletal muscle metmyoglobin was purchased from Sigma (M-0380) and purified by column chromatography on Sephadex G-25 and carboxymethylcellulose, using a pH 6.9, 0.01 M phosphate buffer to load the column and elute the fast bands and a pH 7.1, 0.025 M phosphate buffer to remove the main band. The solution was then concentrated to 10 mM by pressure dialysis against pH 7.0, 0.1 M sodium phosphate buffer. This same buffer was used for preparing all myoglobin solutions. The BuNC solutions were prepared by adding BuNC to degassed buffer and anaerobically adding this buffer and the metmyoglobin stock to enough solid sodium dithionite (Virginia Chemicals) to make the final solution 5 mM in dithionite. The final myoglobin concentrations were approximately 175 μM. These solutions were anaerobically introduced into cuvettes of 0.34-mm path length (Wilmad WG-814 flat EPR cells), which were sealed with wax and varnish.

Transient absorption spectra following photodissociation were measured at room temperature (20–22 °C) by using the instrument described elsewhere (Hofrichter et al., 1983, 1985; Henry et al., 1983). It employs the 532-nm second harmonic (10 ns fwhm) of one neodymium:YAG laser to photolyze a small region of the solution and as a measuring source the broad band emission of a dye (10 ns fwhm) excited by the 355-nm third harmonic of a second neodymium:YAG laser. The dye is stilbene 420 (Exciton Chemical Co.) in methanol, which emits in the range 395–475 nm. Dispersion and detection are achieved with a low-resolution spectrograph, silicon vidicon tube, and optical multichannel analyzer. A reference beam is generated by focusing an image of the dye source inside an unphotolyzed region of the sample and dispersing it onto an adjacent region of the vidicon tube using the sample optics that focus the beam passing through the photolyzed region of the sample. The measured spectra are photolyzed-minus-unphotolyzed difference spectra at various time delays between firing the excitation and probe lasers. Typically, each spectrum is obtained by averaging the results from 9 to 36 laser shots, with a minimum delay of 100 ms between successive shots.

In order to monitor changes in the free BuNC concentration, as well as other possible slow changes in either the sample or

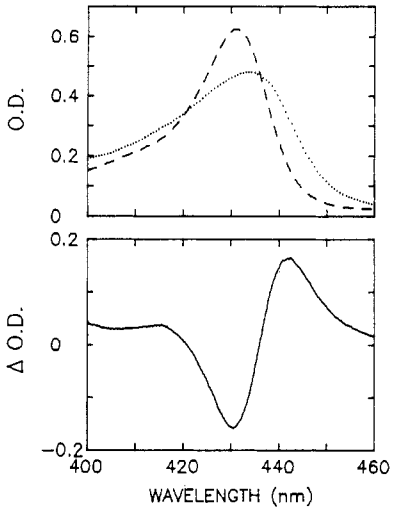

FIGURE 1: Absorption spectra of Mb and MbBuNC. (a) Absolute spectra. The dashed curve is the MbBuNC spectrum, and the solid curve is the Mb spectrum. (b) The difference spectrum Mb − MbBuNC.

the spectrometer, the time delays were chosen in a pseudo random order. In addition, spectra at one arbitrary time delay (1 μs) were measured repeatedly during the course of each experiment in order to ascertain directly whether any drift could be assigned to changes in the sample. A slow decrease in the amplitude of the difference spectrum at 1 μs was observed in some of the experiments, particularly at low BuNC concentrations. This effect was ascribed to the slow decomposition of BuNC mentioned above, and the amplitudes of all of the difference spectra were corrected by using a linear fit to the amplitudes of the 1-μs spectra (plotted as a function of time after sample preparation) to correct the amplitude of each measured spectrum to a constant BuNC concentration.

A typical experiment generated 70–110 difference spectra at different time delays between the photolysis and probe laser pulses. The spectra were processed by singular value decomposition (SVD) (Golub & Reinsch, 1970; Shrager & Hendler, 1982; Hofrichter et al., 1983, 1985). Mathematically, the SVD of a data matrix **A** consisting of n spectra measured at m different wavelengths is defined as $\mathbf{A} = \mathbf{USV}^T$, where **U** is an $m \times n$ matrix in which the columns of **U** form an orthonormal set of m-dimensional vectors (the basis spectra), **S** is an $n \times n$ diagonal matrix of elements called singular values, which serve to scale the normalized basis spectra to each other, and **V** is an $n \times n$ unitary matrix in which the columns of **V** (i.e., rows of $\mathbf{V}^T$) are the time courses of the amplitudes of each of these basis spectra. This procedure transforms the observed set of difference spectra into a set of orthonormal basis spectra. The first basis spectrum is the best least-squares fit to the observed set of difference spectra. The second SVD basis spectrum is orthogonal to the first and, along with the first, gives the best two-component least-squares fit to the observed spectra. The total number of SVD basis spectra is equal to the number of measured difference spectra. This complete SVD set is identical in informational content to the experimental set of difference spectra. However, almost all of the useful information is contained in the first few SVD components. The higher SVD components usually describe noise, and may be discarded with no loss of useful information. Therefore, the SVD procedure determines the minimum number of orthogonal basis spectra (and thus the minimum number of chemical species) needed to describe the data, as well as producing the time dependence of the amplitudes of each of these basis spectra.

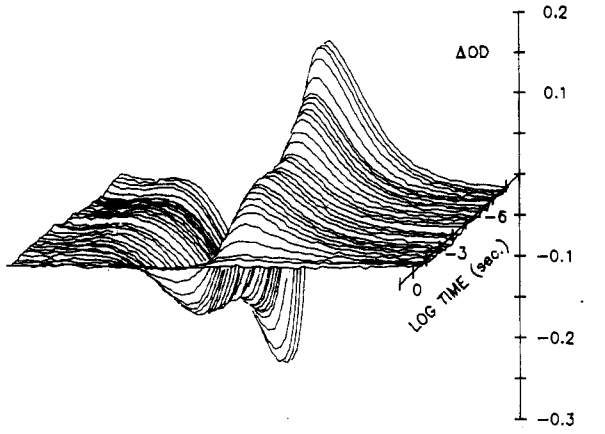

FIGURE 2: Subset of the data measured at 7.8 mM BuNC. A series of 32 time-resolved spectra is shown as a function of the logarithm of the time.

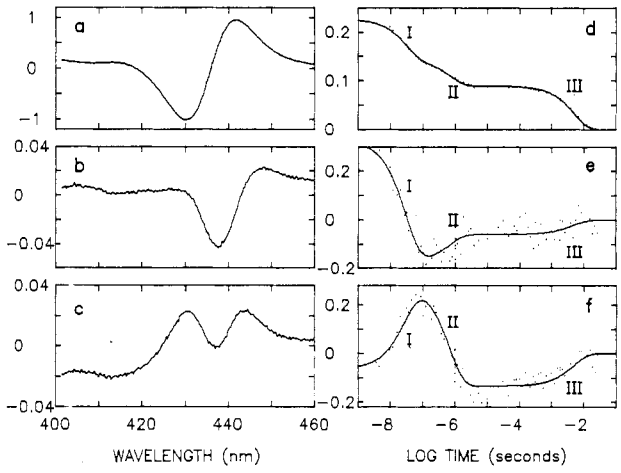

FIGURE 3: Results of an SVD analysis on the MbBuNC data set shown in Figure 2. (a–c) The basis spectra obtained from the SVD analysis of the data set. These basis spectra are scaled by their respective singular values: $S_1 = 6.807$, $S_2 = 0.216$, and $S_3 = 0.200$. (a) The first basis spectrum (**U**·**S** col 1). (b) The second basis spectrum (**U**·**S** col 2) (note expanded scale). (c) Third basis spectrum (**U**·**S** col 3). (d–f) Time dependences of the three basis spectra. The experimental data are shown (···), together with the simultaneous least-squares fit (solid line) to three exponential relaxations for each column of **V** (row of $\mathbf{V}^T$). In the simultaneous fitting procedure, the time dependences were weighted by the singular value associated with each basis spectrum. The Roman numerals I–III designate the $1/e$ times for each of the three relaxations included in the fit.

RESULTS

Soret absorption spectra for Mb and MbBuNC are shown in Figure 1. The absorption maximum of MbBuNC is at 431 nm, while that of Mb is at 434 nm. The overlap between the two spectra decreases the amplitude of the Mb − MbBuNC difference spectrum by a factor of about 2 relative to that for Mb − MbCO, but because the spectrum of MbBuNC is much sharper than that of Mb, there is still a large spectral difference associated with ligand binding.

A portion of a data set in which MbBuNC was photolyzed at a BuNC concentration of 7.8 mM is shown in Figure 2. The amplitude of the difference spectrum decays from that observed for the photoproduct at 10 ns to zero at about 30 ms. A shift in the position of the maximum in the absorption spectra of Mb measured at early times relative to those measured just prior to the final ligand rebinding phase is also barely discernible. The results of the SVD analysis of this experiment are shown in Figure 3. There are three significant SVD basis spectra, as judged by the autocorrelation of each

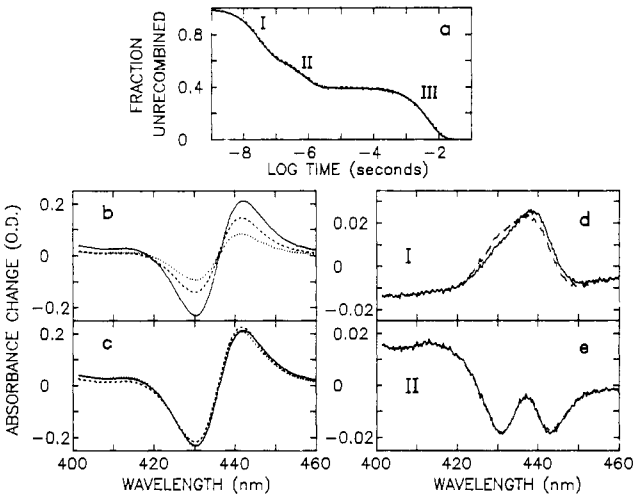

FIGURE 4: Ligand binding curve and spectra reconstructed from SVD analysis. (a) Ligand rebinding curve. The amplitude of V_1 is plotted as the dashed line, and the renormalized (see text) ligand binding curve is plotted as the solid line. (b) Difference spectra reconstructed from the SVD analysis of Figure 3. The unbroken curve corresponds to the immediate photoproduct, the dashed curve to the photoproduct prior to relaxation II, and the dotted curve to the photoproduct prior to relaxation III. (c, d) The differences between spectra which have been normalized to compensate for the effect of geminate recombination. (c) The dashed curve is the change in the spectrum of the deoxy photoproduct that results from relaxation I, calculated without renormalization. The solid curve is the spectral change calculated after renormalization (see text). (d) The dashed curve is the change in the spectrum of the photoproduct that results from relaxation II, calculated without renormalization. The solid curve is the spectral change calculated after renormalization of the ligand binding curve.

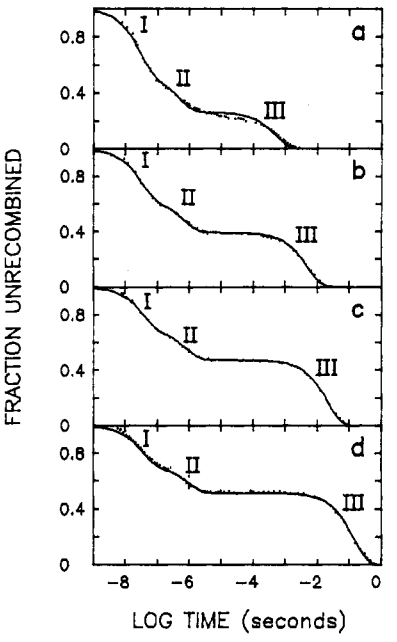

FIGURE 5: Dependence of ligand rebinding curves on BuNC concentration. Panels a–d show ligand rebinding curves, obtained from the amplitude of the first SVD basis spectrum (V col 1) (···) together with the fits using three exponential relaxations (—). The BuNC concentrations are (a) 56, (b) 7.8, (c) 1.7, and (d) 0.15 mM.

component's time dependence (rows of $\mathbf{V}^T$). The first SVD basis spectrum has by far the largest singular value (S_1 = 6.807) and appears similar to a Mb-minus-MbBuNC difference spectrum (Figure 1). The other two basis spectra have more complicated shapes and much lower singular values: S_2 = 0.216 and S_3 = 0.200. Three independent observations argue that the amplitude of basis spectrum 1 should provide a good first approximation to the ligand binding curve. First, basis spectrum 1 closely resembles the static Mb − MbBuNC difference spectrum (Figure 1). Second, ligand binding to Mb is expected to produce much larger changes in the absorption spectrum than arise from conformational changes between Mb species. The magnitude of S_1 is about 20 times greater than the sum of S_2 and S_3. Hence, most of the amplitude of the first basis spectrum is expected to arise from differences in fractional saturation between photolyzed and unphotolyzed species. Third, if the amplitudes of the observed spectra at 430 nm (a peak in the static Mb − MbBuNC difference spectrum and a wavelength at which other spectral changes are small) are compared with the amplitude of $\mathbf{V}_1$, the scaled progress curve superimposes on $\mathbf{V}_1$.

To parametrize the kinetics of ligand rebinding and spectral changes, the time-dependent amplitudes (V_1, V_2, and V_3) of the three basis spectra (U_1, U_2, and U_3) were fitted by using a sum of three exponential relaxations, where the rate constant for each relaxation was constrained to be the same for each basis spectrum. The $1/e$ times for these relaxations, labeled I–III in Figure 3, are 30 ns, 700 ns, and 5 ms. By use of the coefficients obtained from these fits, the SVD basis spectra were added together to give the difference spectrum prior to each of the three relaxations. The ligand rebinding curve obtained from the data in Figure 3 is shown in Figure 4a. The spectra of the photoproduct prior to each of the three relaxations are shown in Figure 4b. If we now assume that the time course of basis spectrum 1 provides a good measure of the population of deoxyhemes, then the spectra of the photoproduct prior to each relaxation can be normalized for ligand recombination. In order to visualize the differences between the normalized spectra of these three species, double-difference spectra were constructed by subtracting the normalized spectrum prior to the second relaxation from that of the immediate photoproduct (Figure 4c) and that before the third relaxation from that prior to the second (Figure 4d). The spectral change observed in the first relaxation (Figure 4c) appears to be a strengthening, sharpening, and red shifting of the deoxymyoglobin spectrum. During the second transition, the spectral change is more complex and could contain contributions from spectral changes in both the deoxy photoproduct and the religanded molecule.

In the presence of spectral changes in either the liganded or deoxy species, the time dependence of the first basis spectrum only provides a first approximation to the true ligand rebinding curve. If the spectral changes are large, the errors in computing the difference spectra of the photoproduct shown in Figure 4d,e become significant. We have recently developed a procedure that can be used to produce a second-order correction to the ligand binding curve and thereby correct the errors in the calculated difference spectra (Hofrichter et al., 1985). The dotted spectra shown in Figure 4d,e and the dashed rebinding curve in Figure 4a result from applying this renormalization procedure to the data in Figure 4. Because the spectral changes observed after photolysis of MbBuNC are small, the renormalization has only a very small effect on the calculated spectra, introducing a small shift in the peak position for the spectral difference which occurs in relaxation I, and essentially no change in the spectral difference which occurs in relaxation II. Because the corrections are small, we will confine the remainder of our analysis to the spectra calculated without applying this procedure.

To determine the dependence of the three relaxations on BuNC concentration, we carried out a series of experiments at BuNC concentrations between 150 μM and 56 mM (Figure 5). These experiments show that the slowest ligand recom-

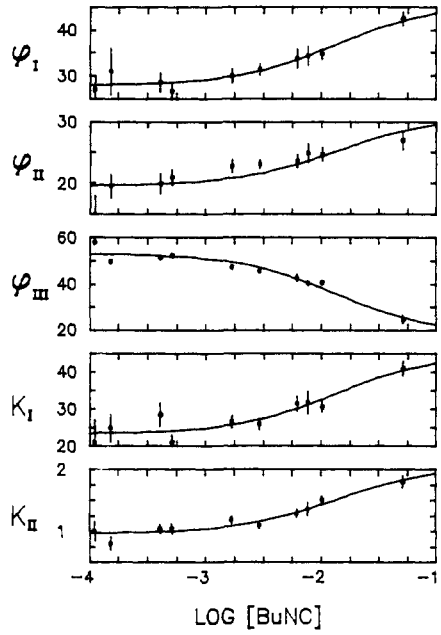

FIGURE 6: Dependence of the geminate rebinding kinetics on BuNC concentration. The points (with error bars) represent the simultaneous exponential fit coefficients to the time-dependent amplitudes of the first SVD basis spectrum as a function of BuNC concentration. ϕ_I is the yield of the first geminate process (relaxation I), and ϕ_{II} is the yield of the second geminate process (relaxation II). Since the first SVD component corresponds closely to ligand recombination, these values closely approximate the geminate recombinational yields. k_I and k_{II} are the corresponding rate constants. Also shown is $\phi_{III} = 1 - (\phi_I + \phi_{II})$, which is the yield for bimolecular recombination. The solid line in each panel is obtained from a simultaneous fit of ϕ_I, ϕ_{II}, k_I, and k_{II} to a simple isotherm describing the binding of BuNC to a non-heme binding site in myoglobin. Each parameter, x, is calculated by using $x(c) = x_A f_A + x_B(1 - f_A)$, with $f_A = 1/(1 + K_A c)$, where A denotes Mb and B denotes the complex of Mb + BuNC, K_A is the association constant for the formation of this complex, and c is the BuNC concentration.

bination process (relaxation III) is definitely bimolecular, with the rate slowing in proportion to the decreasing BuNC concentration and the process becoming nonexponential at low BuNC concentrations. When independently prepared 7 mM BuNC solutions were used, a bimolecular rate constant (k_{III}) of $2.7 \pm 0.3 \times 10^4$ M^{-1} s^{-1} was obtained. This is to be compared with published values of 5.0×10^4 M^{-1} s^{-1} (Olson & Gibson, 1971), 3.7×10^4 M^{-1} s^{-1} (Stetzkowski et al., 1979), and 2.8×10^4 M^{-1} s^{-1} (Mims et al., 1983). Olson & Gibson (1971) observed no dependence of the bimolecular rate constant on BuNC concentration over a range of concentrations from 0.05 to 0.3 mM in stopped-flow experiments and measured the identical rate constant in photolysis experiments at about 1 mM. As our value of 2.7×10^4 M^{-1} s^{-1} agrees well with these literature values taken at lower BuNC concentrations, we have used this concentration-independent rate constant to determine the BuNC concentrations for the remainder of the data sets (see Materials and Methods).[2]

The amplitudes and rates for ligand rebinding in relaxations I and II do not scale linearly with concentration and are thus not bimolecular. As the BuNC concentration is increased

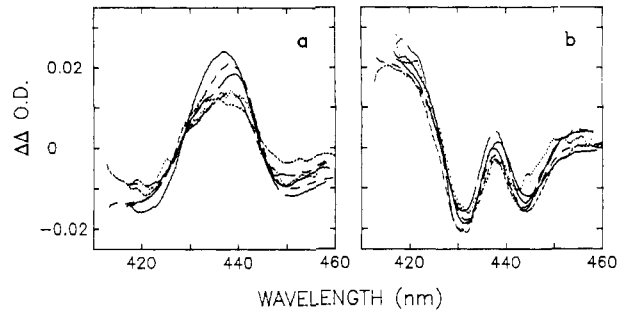

FIGURE 7: Concentration dependence of spectral changes associated with relaxations I and II. The difference spectra prior to each relaxation were first normalized to 100% Mb using the ligand binding amplitudes obtained from fits to V_1. The spectrum before each relaxation was then subtracted from the spectrum after the relaxation to give a double-difference spectrum. The resulting spectra were then normalized to account for the variations in sample concentration and path length. This normalization procedure correctly calculates the change in the Mb spectrum that accompanies each relaxation if it is assumed that the changes take place only in the deoxy species. (a) Comparison of deoxy spectral changes for relaxation I. (b) Comparison of spectral changes (assumed deoxy) for relaxation II. The BuNC concentrations depicted by the curves are (—) 10.2, (——) 7.15, (--) 1.68, (---) 0.51, (·--) 0.41, and (···) 0.15 mM.

40-fold, k_I changes by 50%, k_{II} by 70%, ϕ_I by 45%, and ϕ_{II} by 20%. The rates and amplitudes for these rebinding reactions are plotted in Figure 6. This weak concentration dependence is most easily explained by assuming that a second molecule of BuNC binds to the protein and alters the geminate parameters. Using this assumption, we have simultaneously fitted the four parameters plotted in Figure 6 to a titration curve for the noncovalent binding of one additional molecule of BuNC[3] and obtained a dissociation constant of about 15 mM. The data in this titration curve are noisy, and multiple binding sites with similar dissociation constants are not precluded (Wishnia, 1969), but the quality of the data does not justify a more detailed analysis. It is clear that neither geminate relaxation phase disappears when the data in Figure 6 are extrapolated to zero or infinite concentration of BuNC. Thus, the species at both limits of BuNC concentration display two geminate recombination phases.

Analysis of the time courses of the basis spectra shows that at all BuNC concentrations the spectral changes and ligand recombination occur simultaneously. Over 10 experiments, the rate constants obtained from separate fits to the amplitudes (V_2 and V_3) of the individual basis spectra U_2 and U_3 are generally identical, within the combined standard error, with those of the simultaneous fits to V_1, V_2, and V_3 which are dominated by the relaxation times for ligand rebinding (V_1). The few times when the rate constants from the separate fits differed from those from the simultaneous fit by more than the combined standard errors, the amplitudes associated with the anomalous rates were generally small. Finally, there was no trend among the experiments for the rate constants obtained

[2] The dependence of the geminate parameters ϕ_I and ϕ_{II} on BuNC concentration together with the four-species model (eq 3) predicts that the bimolecular rate constant would increase by a factor of 2 at high BuNC concentration, if k_{43} is assumed to be concentration independent. The BuNC concentrations determined by assuming a fixed value for the bimolecular rate constant are therefore potentially in error by a comparable factor.

[3] A model of the sort suggested by eq 2 predicts that the geminate decays will be biexponential when the titration site is partially occupied. However, a curve consisting of two exponential relaxations may be satisfactorily fit by a single exponential with a rate which is the amplitude-weighted average of the rate constants. For instance, the fit of a single exponential to a curve that is the sum of two exponential relaxations of equal amplitudes and rate constants differing by a factor of 2 gives a relaxation rate that is less than 10% smaller than the average of the two rate constants, with root mean square deviations in the fitted curve of less than 1%. Since both geminate rate constants varied by less than a factor of 2 over the entire concentration range, only a single relaxation rate could be obtained for each of the geminate processes in each experiment.

from the fits to V_2 or V_3 to be either faster or slower than those obtained from the simultaneous fits. Figure 7 shows the spectral changes accompanying relaxations I and II at the various BuNC concentrations. For relaxation I there is a decrease in the amplitude of the spectral change as the concentration of BuNC decreases which roughly parallels the concentration dependence of the geminate parameters in Figure 6. The spectral change accompanying relaxation II appears to be independent of BuNC concentration.

Discussion

Three ligand rebinding phases are observed after photodissociation of MbBuNC (Figure 4). Measurement of the dependence of the amplitudes and relaxation times on BuNC concentration shows that the slowest phase is bimolecular (relaxation III), while the two faster phases (relaxations I and II) result from geminate recombination. The geminate phases are, however, weakly dependent on the BuNC concentration (Figure 6). This dependence can be explained by assuming that there is at least one additional weak binding site for the noncovalent attachment of BuNC to Mb. The noncovalent binding of BuNC both increases the geminate yields and decreases the relaxation times for the two geminate phases. For phase I, binding of the additional BuNC molecule increases the geminate yield from 0.28 to 0.46 and decreases the relaxation time from 43 to 22 ns, while for phase II the geminate yield increases from 0.20 to 0.31, and the relaxation time decreases from 1 μs to 500 ns. Weak binding of xenon (Schoenborn, 1967) and the nonpolar molecules pentane and butane (Wishnia, 1969) to Mb has been demonstrated previously. The dissociation constants for the hydrocarbons range from 1 to 7 mM, comparable to, but somewhat smaller than, the value of 15 mM obtained for BuNC from the fit to our data shown in Figure 6.

There are, as yet, no experiments on MbBuNC with time resolution better than about 10 ns, so it is possible that there is a subnanosecond geminate recombination phase that cannot be detected in the present experiments. From experiments in which MbBuNC was partially photolyzed with a 150-μs flash, Brunori et al. (1973) derived a quantum yield for photodissociation of 0.32. If we assume a primary photochemical quantum yield of unity for breaking the iron–ligand bond, our results (Figure 6) predict a yield ($1 - \phi_I - \phi_{II}$) of 0.52 at the BuNC concentration [0.5 mM (M. Brunori, private communication)] used in the quantum yield experiments. For consistency, these results would require that the 10-ns quantum yield be 0.6. The difference between this value and unity could arise from either the existence of a subnanosecond geminate recombination phase or a photochemical quantum yield less than unity for breaking the iron–ligand bond.

The results on geminate recombination for MbBuNC may be compared with those for MbO_2 and MbCO. For MbO_2, a geminate phase has been seen in the nanosecond time regime, with a relaxation time of 55 ns and a yield of 27% (Duddell et al., 1980), and the existence of a subnanosecond rebinding phase (relaxation time 100 ps; yield about 80%) has also been reported (Martin et al., 1982). For MbCO, a single geminate phase has been seen, with a yield of only 4% and relaxation time of 180 ns (Henry et al., 1983). There are two possible ways in which the results for BuNC could be aligned with those for the diatomic ligands. One possibility is that the nanosecond geminate phases for MbO_2 and MbCO correspond to relaxation II for MbBuNC, while geminate phase I is much more rapid for the diatomic ligands and can perhaps be identified with the subnanosecond rebinding reported for MbO_2 (Martin et al., 1982). The second possibility is that relaxation II corresponds to rebinding from a protein site that is unique to MbBuNC and does not exist for the diatomic ligands. Relaxation I would then correspond to the nanosecond geminate phases for MbO_2 and MbCO, and possible subnanosecond geminate phases for MbBuNC which have not yet been detected might still correspond to similar phases for the diatomic ligands. The present data cannot distinguish between these two possibilities. Relating the data in the latter way is appealing, because the existence of the additional binding site can be naturally rationalized as resulting from the large size of the BuNC ligand.[4] One can readily envisage an additional barrier for motion of the large ligand inside the protein that does not exist for the diatomic ligands.

Table I: Rate Constants Calculated Using Sequential Models for Ligand Rebinding to Myoglobin

	ligand		
	BuNC[a]	O_2[b]	CO[b]
rates for intraprotein processes (μs^{-1})			
k_{21}	6.6	4.9	0.23
k_{23}	17	13	5.2
k_{32}	0.95		
k_{34}	0.71		
rates for ligand entry into protein ($M^{-1}\ s^{-1}$)	0.1×10^6	80×10^6	17×10^6

[a] Rate constants calculated by using eq 4 and 5 derived for the four-species model (eq 3) with values for ϕ_I, ϕ_{II}, k_I, and k_{II} obtained by extrapolating the fits described in Figure 6 to zero [BuNC], and the value for $k_{on} = 2.7 \times 10^4\ M^{-1}\ s^{-1}$ obtained in this work. [b] Rate constants taken from Table I of Henry et al. (1983) calculated by using the three-species model (eq 2).

In order to explain the biphasic geminate rebinding curve for BuNC and the accompanying spectral changes, a model is required that includes a minimum of four species. We have chosen to discuss the results in terms of a four-species sequential model despite the fact that we clearly cannot rule out a variety of more complex models. This simple model has the form:

$$\underset{1}{\text{MbBuNC}} \underset{k_{21}}{\overset{k_{12}}{\rightleftharpoons}} \underset{2}{\text{Mb:BuNC}} \underset{k_{32}}{\overset{k_{23}}{\rightleftharpoons}} \underset{3}{\text{Mb::BuNC}} \underset{k_{43}}{\overset{k_{34}}{\rightleftharpoons}} \underset{4}{\text{Mb + BuNC}} \quad (3)$$

We define ϕ_2 as the probability that a molecule initially in state 2 returns to state 1 and ϕ_3 as the corresponding probability for state 3. If we now assume that $k_{21}, k_{23} \gg k_{32}, k_{34} \gg k_{12}, k_{43}[\text{BuNC}]$, then we can invoke the steady-state assumption for the intermediates in the rebinding of ligands from states 3 and 4. The expressions for ϕ_2 and ϕ_3 are then given by

$$\phi_2 \simeq k_{21}/(k_{21} + k_{23}) \qquad \phi_3 \simeq k_{32}\phi_2/(k_{34} + k_{32}\phi_2) \quad (4)$$

and the measured kinetic parameters are related to the rate constants of the model by

$$\begin{gathered} k_I \simeq k_{21} + k_{23} \qquad k_{II} \simeq k_{34} + k_{32}\phi_2 \\ k_{on} \equiv k_{III}/[\text{BuNC}] \simeq k_{43}\phi_3 \\ k_{off} \simeq k_{12}(1 - \phi_2)(1 - \phi_3) \qquad \phi_I \simeq \phi_2 \\ \phi_{II} \simeq \phi_3(1 - \phi_2) \end{gathered} \quad (5)$$

[4] An intriguing speculation is that one of the ligand binding sites in the protein involved in geminate rebinding may correspond to the noncovalent binding site which is responsible for the concentration dependence of the geminate kinetics. This hypothesis was disproven by a mixed-ligand experiment, in which MbCO was photodissociated in the presence of high concentrations of BuNC. Insignificant fast ($\tau < 1\ \mu s$) binding of BuNC was observed, which demonstrates that any noncovalently bound BuNC is not on the reaction pathway.

The rate constants calculated for this model at low BuNC concentrations where the weak non-heme binding site is unoccupied are given in Table I, together with the values obtained by using the three-species model (eq 2) to analyze the binding of CO and O_2 to myoglobin (Henry et al., 1983). The rate k_{23} for BuNC is similar to the corresponding values for CO and O_2, which are the rates at which these ligands escape from the heme pocket. The rate of rebinding to the heme from state 2, k_{21}, is also similar to that observed for O_2, reflecting the similar rates and geminate yields for relaxation I for BuNC and O_2. The much smaller rate for CO binding at the heme is the primary reason for the much smaller geminate yield observed for this molecule. These results appear to support the second alignment of the BuNC processes discussed above, in which state 2 corresponds to BuNC bound in the heme pocket, state 3 corresponds to Mb containing BuNC bound in a different site or sites, and state 4 is relaxed Mb + BuNC. The large values of ϕ_2 and ϕ_3 are difficult to rationalize in terms of the conclusion of Mims et al. (1983) that most of the differences between the equilibrium binding constants for CO and isocyanides result from specific steric interactions with residues on the distal side of the heme binding site. On the basis of their analysis these interactions could be expected to significantly decrease k_{21} and ϕ_2 for BuNC relative to CO. No alignment of the kinetic data is consistent with this prediction since both k_{21} and k_{32} for BuNC are faster than k_{21} for CO.

In contrast, the rate at which BuNC enters the protein (k_{43}) is reduced by over a factor of 100 relative to the corresponding rates for CO and O_2 (k_{32}). This difference argues that there is an unfavorable interaction between the protein matrix and BuNC at the transition state for the entry step which does not exist for CO and O_2. This result is consistent with the recent conclusions of Calhoun and co-workers from fluorescence quenching experiments on liver alcohol dehydrogenase and alkaline phosphatase. These studies showed that O_2 was able to enter the protein and diffuse rather freely through the protein matrix (Calhoun et al., 1983a) but that other small molecules such as acrylamide and acetone could not quench buried tryptophan fluorescence and apparently were very efficiently excluded from the interior of the protein (Calhoun et al., 1983b).

If binding constants to the protein are calculated from the kinetic data with the assumption that the heme binding site is blocked, the values are 3.3 M^{-1} for CO, 6.2 M^{-1} for O_2, and only 0.15 M^{-1} for BuNC. These values suggest that, relative to the diatomic ligands, BuNC is excluded from the protein matrix with a free energy of about 2 kcal/mol. In the analysis of Mims et al. (1983) it was assumed that a myristyltrimethylammonium micelle was a good model for the protein matrix and, on the basis of this assumption, the predicted ratio of the binding constants for CO and BuNC was 0.12 (the ratio of the partition coefficients for these ligands between soap micelles and aqueous solutions). Mims et al. (1983) argue that most of the difference in the affinity of Mb for CO and BuNC results from unfavorable interactions between the alkyl chain and specific residues in the heme pocket, particularly the distal histidine, which amount to a total of 3.6 kcal/mol. The only scheme in which our data are consistent with this analysis is one in which it is assumed that both species 3 and species 2 have BuNC bound in the heme pocket in a conformation closely resembling the geometry of the bound ligand. In this scheme the interactions between BuNC and the heme pocket described by Mims et al. (1983) would also decrease the rate at which the ligand binds to the protein matrix (k_{43}). Relaxation I could, however, not be ascribed to ligand motion but would have to result from some other relaxation, presumably on the proximal side of the heme. If this scheme is incorrect and species 3 in our model does not have the BuNC ligand positioned very close to its bound position in the heme pocket, then roughly 3 kcal of the total 3.6-kcal difference in the binding energies of CO and BuNC results directly from their assumption that the partition coefficients for the two ligands are identical with those for the heme–micelle system.

A more straightforward explanation of our result is that the larger ligand is excluded from the protein as the net result of a number of competing thermodynamic contributions to the binding constant (partition coefficient). In addition to the hydrophobic interactions between the ligand and water and the loss in translational entropy ("cage effect") discussed by Mims et al., these may also include a general disruption of protein–protein interactions by the bulky ligand and stabilization of the isocyanide in water by dipole–dipole interactions. For the small diatomic ligands all of these contributions to the partition coefficient are small, and these ligands are able to diffuse through the protein with only very minor deviations from the equilibrium protein conformation, similar to the mobile defects hypothesis of Lumry & Rosenberg (1975). The bulky, polar BuNC, on the other hand, must lose unfavorable hydrophobic interactions, favorable electrostatic interactions with the solvent, and translational entropy when it enters the protein. It may also distort the protein from its equilibrium folded form without generating sufficient stabilizing interactions to compensate for the lost protein–protein interactions. The net result is that, relative to CO and O_2, the protein partitions against BuNC, instead of for BuNC as observed for micelles, and both the equilibrium binding constant and the rate of binding are significantly decreased.

The decrease in k_{43} for BuNC may also provide a clue to the origin of the second geminate phase in the dissociation of BuNC from myoglobin. This phase could be explained as arising from the same kinetic barrier that decreases the rate at which the ligand enters the protein. If the pathway is reversible, as assumed in writing the model (eq 3), then a significant increase in the lifetime of state 3, resulting from an increase in the free energy of the transition state between states 3 and 4, could increase the geminate yield from this state from a level that is undetectable for O_2 and CO to the levels observed for BuNC.

Another major difference between MbBuNC and the complexes with the diatomic ligands is that spectral changes are observed subsequent to photodissociation. In the case of MbCO the spectrum at 30 ns after photodissociation was identical with that of Mb at equilibrium (Henry et al., 1983). Preliminary experiments on MbO_2 gave similar results (Sommer et al., 1983).[5] Independent fitting to the kinetics of ligand rebinding and spectral changes shows that the relaxation times for the spectral changes in MbBuNC are indistinguishable from the relaxation times for geminate recombination and must be viewed as occurring simultaneously.

The spectral changes observed in relaxations I and II are considerably smaller than those that have been associated with tertiary structural changes in Hb (Hofrichter et al., 1983, 1985). Their small amplitudes, as well as problems resulting from imperfect normalization for the fraction of liganded molecules, make it difficult to precisely determine the wavelength dependence of the spectral changes. Despite these

[5] A very small spectral change was observed with an apparent relaxation time of less than 20 ns for both ligands, but it was not possible to rule out an optical artifact as the source of this spectral change.

problems, it is clear that the spectral changes accompanying relaxations I and II are quite different. The difference spectrum in relaxation I could result simply from a sharpening of the spectrum of Mb, with very little contribution from the spectrum of the liganded molecules. The difference spectrum in relaxation II, however, is very difficult to rationalize as arising from changes only in the deoxy species but could be explained as arising from a shift of the spectra of both the deoxy and the liganded photoproducts. A second qualitative difference in the nature of the two conformational changes is the finding that the spectral change associated with relaxation I depends on BuNC concentration, while the spectral change associated with relaxation II is essentially concentration independent.

The simplest model for the spectral changes in the deoxy species is that the photodissociated ligand distorts the Mb conformation and that the detailed changes in the conformation of the heme pocket depend on the location of the ligand within the protein. When the ligand moves from its position in species 2 to its position in species 3, the protein rapidly relaxes into a different conformation. When the ligand leaves the protein in relaxation II, the structure of the deoxy molecule again relaxes to that of Mb at equilibrium. No such change is observed with CO or O_2, presumably because they are much smaller, and can be accommodated by the transient holes created in the protein by fluctuations about the ligand-free Mb conformation.

The most straightforward explanation of the spectral change in the liganded molecules is that the spectrum of the MbBuNC formed by rebinding in relaxation II is different from that of MbBuNC at equilibrium. This interpretation of the observed spectral changes is consistent with the four-species model (eq 3) which argues that the deoxy species to which the ligand is binding is structurally different from the immediate photoproduct and from Mb at equilibrium, having undergone a conformational change in relaxation I. This interpretation raises a different problem, however, because it requires that the altered spectrum of the liganded molecules relax to the equilibrium liganded spectrum at some time after relaxation II. In the data sets at the highest BuNC concentrations, there is a hint of a spectral change occurring subsequent to relaxation II at about 100 μs. Our data are not sufficiently consistent to demonstrate the existence of this relaxation unambiguously, and the alternative possibility that the liganded spectrum recovers at times longer than 0.1 s cannot be ruled out. Clearly there are other models that could also explain the observation of two different spectral relaxations but are less consistent with the data. For example, one could argue that multiple conformations of either the parent MbBuNC molecules or the immediate photoproduct are responsible for the two observed relaxations. This explanation is inconsistent with our interpretation of the spectral change in relaxation I as arising exclusively from the spectrum of the deoxyhemes, since, if relaxation I arose from geminate rebinding to one of the two conformers, then its liganded spectrum should also differ from that of the unphotolyzed sample.

The observation of an altered spectrum for the liganded myoglobin formed in relaxation II has important consequences for the development of a detailed pathway for ligand binding to Mb. This result suggests that the heme–ligand bond is formed in a molecule prior to its relaxation to the equilibrium liganded tertiary structure. It therefore appears that the steps of the ligand dissociation pathway which are observed subsequent to the photolysis of the heme–ligand bond may not be directly applicable to the process of ligand binding, since the protein structure encountered by the ligand entering the protein from the solvent may differ significantly from that encountered by a ligand leaving the photodissociated molecule. The observation of tertiary structural changes in liganded myoglobin indicates that tertiary conformational changes in response to ligand motions need not be instantaneous. If this is true, then the ligand dissociation pathway observed in photolysis experiments on other heme proteins [e.g., see Hofrichter et al. (1983, 1985)] may serve to point out the complexity of the detailed ligand binding process but cannot be used to determine the actual rates for the steps of this process.

Acknowledgments

We thank William Eaton for his support and encouragement of this work, John Olson for the gift of several alkyl isocyanide compounds and for his interest in this work, and Attila Szabo for very helpful discussions.

Registry No. BuNC, 2769-64-4.

References

Alben, J. O., Beece, D., Bowne, S. F., Eisenstein, L., Frauenfelder, H., Good, D., Marden, M. C., Moh, P. P., Reinisch, L., Reynolds, A. H., Shyamsunder, E., & Yue, K. T. (1982) *Proc. Natl. Acad. Sci. U.S.A. 79*, 3744–3748.

Antonini, E., & Brunori, M. (1971) *Hemoglobin and Myoglobin in Their Reactions with Ligands*, North-Holland Publishing Co., Amsterdam.

Austin, R. H., Beeson, K. W., Eisenstein, L., Frauenfelder, H., & Gunsalus, I. C. (1975) *Biochemistry 14*, 5355–5373.

Beece, D., Eisenstein, L., Frauenfelder, H., Good, D., Marden, M. C., Reinisch, L., Reynolds, A. H., Sorensen, L. B., & Yue, K. T. (1980) *Biochemistry 19*, 5147–5157.

Brunori, M., Giacometti, G. M., Antonini, E., & Wyman, J. (1973) *Proc. Natl. Acad. Sci. U.S.A. 70*, 3141–3144.

Calhoun, D. B., Vanderkooi, J. M., Woodrow, G. V., & Englander, S. W. (1983a) *Biochemistry 22*, 1526–1532.

Calhoun, D. B., Vanderkooi, J. M., & Englander, S. W. (1983b) *Biochemistry 22*, 1533–1539.

Case, D. A., & Karplus, M. (1979) *J. Mol. Biol. 132*, 343–368.

Chance, B., Fischetti, R., & Powers, L. (1983) *Biochemistry 22*, 3820–3829.

Cornelius, P. A., Steele, A. W., Chernoff, D. A., & Hochstrasser, R. M. (1981) *Proc. Natl. Acad. Sci. U.S.A. 78*, 7526–7529.

Cornelius, P. A., Hochstrasser, R. M., & Steele, A. W. (1983) *J. Mol. Biol. 163*, 119–128.

Dlott, D. D., Frauenfelder, H., Langer, P., Roder, H., & DiIorio, E. (1983) *Proc. Natl. Acad. Sci. U.S.A. 80*, 6239–6243.

Doster, W., Beece, D., Bowne, S. F., DiIorio, E. E., Eisenstein, L., Frauenfelder, H., Reinisch, L., Shyamsunder, E., Winterhalter, K. H., & Yue, K. T. (1982) *Biochemistry 21*, 4831–4839.

Duddell, D. A., Morris, R. J., Muttucumaru, N. J., & Richards, J. T. (1980) *Photochem. Photobiol. 31*, 479–484.

Frauenfelder, H., Petsko, G. A., & Tsernoglou, D. (1979) *Nature (London) 280*, 558–563.

Friedman, J. M., Stepnoski, R. A., Stavola, M., Ondrias, M. R., & Cone, R. L. (1982) *Biochemistry 21*, 2022–2028.

Golub, G. H., & Reinsch, C. (1970) *Numer. Math. 14*, 403–420.

Hasinoff, B. B. (1977) *Arch. Biochem. Biophys. 183*, 176–188.

Hasinoff, B. B. (1981) *J. Phys. Chem. 85*, 526–531.

Henry, E. R., Sommer, J. H., Hofrichter, J., & Eaton, W. A. (1983) *J. Mol. Biol. 166*, 443–451.

Hofrichter, J., Sommer, J. H., Henry, E. R., & Eaton, W. A. (1983) *Proc. Natl. Acad. Sci. U.S.A. 80*, 2235–2239.
Hofrichter, J., Henry, E. R., Sommer, J. H., Deutsch, R. D., Ikeda-Saito, M., Yonetani, T., & Eaton, W. A. (1985) *Biochemistry 24*, 2667–2679.
Lumry, R., & Rosenberg, A. (1975) in *L'eau, Et Les Systemes Biologiques* (Alfen, A., & Berteaud, A. J., Eds.) pp 53–61, Centre National de Recherche Scientifique, Paris.
Martin, J. L., Migus, A., Poyart, C., Lecarpentier, Y., Antonetti, A., & Orszag, A. (1982) *Biochem. Biophys. Res. Commun. 107*, 803–810.
Martin, J. L., Migus, A., Poyart, C., Lecarpentier, Y., Astier, R., & Antonetti, A. (1983) *Proc. Natl. Acad. Sci. U.S.A. 80*, 173–177.
Mims, M. P., Porras, A. G., Olson, J. S., Noble, R. W., & Peterson, J. A. (1983) *J. Biol. Chem. 258*, 14219–14232.
Olson, J. S., & Gibson, Q. H. (1971) *J. Biol. Chem. 246*, 5241–5253.
Olson, J. S., McKinnie, R. E., Mims, M. P., & White, D. K. (1983) *J. Am. Chem. Soc. 105*, 1522–1527.
Reynolds, A. H., & Rentzepis, P. M. (1982) *Biophys. J. 38*, 15–18.
Reynolds, A. H., Rand, S. D., & Rentzepis, P. M. (1981) *Proc. Natl. Acad. Sci. U.S.A. 78*, 2292–2296.
Schoenborn, B. P. (1967) *Nature (London) 214*, 1120–1122.
Shrager, R. I., & Hendler, R. W. (1982) *Anal. Chem. 54*, 1147–1152.
Sommer, J. H., Henry, E. R., Hofrichter, J., & Eaton, W. A. (1983) *Biophys. J. 41*, 8a.
Stetzkowski, F., Cassoly, R., & Banerjee, R. (1979) *J. Biol. Chem. 254*, 11351–11356.
Wishnia, A. (1969) *Biochemistry 8*, 5064–5074.

^{1}H NMR Study of Labile Proton Exchange in the Heme Cavity as a Probe for the Potential Ligand Entry Channel in Myoglobin†

Juliette T. J. Lecomte and Gerd N. La Mar*
Department of Chemistry, University of California, Davis, California 95616
Received March 28, 1985

ABSTRACT: The exchange rates of heme cavity histidine nitrogen-bound protons in horse and dog metcyanomyoglobins have been determined at 40 °C as a function of pH by ^{1}H NMR spectroscopy. They were compared to the results reported for the sperm whale homologue [Cutnell, J. D., La Mar, G. N., & Kong, S. B. (1981) *J. Am. Chem. Soc. 103*, 3567–3572]. The rate profiles suggest that the exchange follows EX_2-type kinetics, and the relative rate values favor a penetration model over a local unfolding model. It was found that the behavior of protons located on the proximal side of the heme is similar in the three proteins. The distal histidyl imidazole NH, however, shows a highly accelerated hydroxyl ion catalyzed rate in horse and dog myoglobins relative to that in sperm whale myoglobin. NMR spectral and relaxational characteristics of the assigned heme cavity protons indicate that the global geometry of the heme pocket is highly conserved in the ground-state structure of the three proteins. We propose a model that attributes the different distal histidine exchange behavior to the relative dynamic stability of the distal heme pocket in dog or horse myoglobin vs. sperm whale myoglobin. This model involves a dynamic equilibrium between a closed heme pocket as found in metaquomyoglobin [Takano, T. (1977) *J. Mol. Biol. 110*, 537–568] and an open pocket as found in phenylmetmyoglobin [Ringe, D., Petsko, G. A., Kerr, D. E., & Ortiz de Montellano, P. R. (1984) *Biochemistry 23*, 2–4]. The greater stabilization of the open pocket in horse and dog myoglobins relative to sperm whale myoglobin is rationalized by the substitution CD3 Arg (sperm whale) → Lys (horse, dog). This residue holds the pocket closed in sperm whale myoglobin via hydrogen bonds to both a heme propionate and Asp E3; the substituted Lys is not capable of forming both of those stabilizing interactions in dog and horse myoglobins. Our results indicate that labile proton exchange of histidine can serve as a general useful probe of the mechanism of interaction between solvent and buried side-chain sites in folded proteins.

Proteins in general, and the oxygen-binding proteins myoglobin and hemoglobin in particular, exhibit a wide range of structural fluctuations about an equilibrium structure (Gurd & Rothgeb, 1979; McCammon & Karplus, 1980; Karplus & McCammon, 1981; Debrunner & Frauenfelder, 1982; McCammon & Karplus, 1983; Woodward et al., 1982; McCammon, 1984) which is essentially that described in the X-ray studies (Perutz & Mathews, 1966; Perutz, 1976; Takano, 1977a,b; Phillips, 1980). Some of the dynamic properties that can be clearly traced to function are the side-chain motions allowing the formation of transient channels through which molecular oxygen enters and leaves the heme cavity (Perutz & Mathews, 1966; Takano, 1977a,b; Case & Karplus, 1979). While there may be several pathways for O_2 entry, a recent X-ray structure of phenyl-ligated metmyoglobin (metMb)[1] (Ringe et al., 1984) has revealed an open "door" to the heme pocket: the reported structural differences with respect to metMbH_2O involve solely the orientation of the

† This research was supported by Grants CHE-81-08766 and CHE-84-15329 from the National Science Foundation.
* Author to whom correspondence should be addressed.

[1] Abbreviations: Mb, myoglobin(s); metMb, metmyoglobin(s); metMbCN, metcyanomyoglobin(s); NMR, nuclear magnetic resonance.

0006-2960/85/0424-7388$01.50/0